DISTRIBUTION STATEMENT A: Approved for public release; distribution is unlimited.

Modeling and Validation of the Effects of Sound on the Marine Environment

Martin Siderius and Scott Schecklman
Portland State University
ECE Department
1900 SW 4th Ave., Suite 160-11
Portland, OR 97201
phone:(503) 725-3223 fax:(503) 725-3807 email: siderius@pdx.edu

Award Number: N000140910485
http://www.pdx.edu

LONG-TERM GOALS

The long-term goals are to develop novel techniques to measure and predict, through modeling, the effect of sound on the marine environment. Modeling includes acoustic sources, propagation and the interaction of sound with animal behavior models. Determining the necessary environmental information such as bathymetry, sound speed and seabed properties for accurate modeling is also an essential component of this work.

OBJECTIVES

The objective of this research is to develop modeling tools for estimating the impact of sound on marine life. The goal is to provide state-of-the-art, open source codes to model sound sources, sound propagation and animal behavior. We are also assembling open source environmental databases for quantities such as seabed properties, bathymetry and ocean sound speed. Together, these tools will provide the best estimate of the impact of various sonar systems on the marine environment. These tools are bundled with a simple user interface in the ESME Workbench and are intended to be a type of gold standard for estimating impact. Currently, Navy environmental impact statements are prepared at the Naval Undersea Warfare Center (NUWC) and by several government contractors. The software and databases being used are often either classified or proprietary. ONR has put together a team consisting Boston University (David Mountain), Biomimetica (Dorian Houser), HLS Research (Michael Porter) and Portland State University (Martin Siderius) to build the ESME Workbench which will make the needed calculations for assessing environmental impact without using classified or proprietary components. In 2010 there were two main areas of research, 1) Quantifying different methods for modeling sonar impact. 2) Developing an Adaptive Mesh Refinement (AMR) algorithm to more quickly assess marine mammal harassments in large volumes of ocean.

APPROACH

Comparison of current methodologies for preparing impact statements

A study was conducted to compare two methodologies for incorporating marine animals into environmental impact calculations and demonstrate the differences between them. In short, marine

mammal impact is estimated by calculating the expected sound pressure level and the animal distributions. Two methods for animal distributions are considered, the first assumes the animals are distributed in depth according to a species dependent histogram. This is a static approach in that it treats the animals as frozen in time at depths corresponding to the histogram. The second method uses simulated animals (animats) which are randomly distributed in an area of interest and their swimming behavior is simulated over time. The static distribution method accounts for a species location in depth by assuming a particular diving behavior for the species. The animal's statistical distribution in depth is generally derived from collected data or using a data-driven animal movement model such as Biomemetica's 3MB. This method contains no time dependence and therefore assumes the mammals remain within sub-volumes of the simulation space.

Comparisons between the animat and static distribution methods were made based on a generalized, range-independent environment which allowed us to study the effects the methodologies without excessively complex environments. The ray/beam code Bellhop [2,3] was used as the acoustic propagation model with the environmental parameters dependent on the specific scenario. A shallow diving and deep diving species were simulated in both shallow and deep ocean environments. For simplicity, the modeling and discussion was limited to Level B harassment due to behavioral disruption and in the absence of auditory fatigue. The number of harassments estimated to occur from an exercise involving mid-frequency sources was calculated by evaluating a risk function that relates the risk of harassment to the maximum sound pressure level (SPL). The risk function varies between 0 (no risk) and 1 (maximum risk) and can be interpreted as the proportion of the time a given individual may alter its behavior in response to a given max SPL [4]. This value was then extrapolated to the population level to give the number of takes in each method.

The study concluded that the two methods do not produce the same result because the static distribution method is not time-dependent. Removal of the temporal component eliminates the potential for an animal to occupy more than one sub-volume and reduces the risk of encountering higher level exposures. Intuitively, this becomes clear if one considers a sound source that ensonifies a small region with an SPL near 195 dB for a very long period of time. The animat method would reveal that (given enough time) eventually *all* of the marine mammals would pass through this high intensity region and be harassed. The static distribution method, on the other hand, would arrive at a smaller, fixed number of harassments based only on the typical volume distribution of the marine mammals.

Approach to Adaptive Mesh Refinement of the simulation space

Often, underwater sound activity includes a number of sources at different frequencies possibly moving on different platforms (e.g. ships) for several hours or days. Calculating the expected SPL for these types of scenarios creates a significant computational burden. The need to run faster simulations motivates us to review some of the underlying analysis assumptions and techniques to see if improvements in efficiency can be achieved.

The Level B non-physiological takes threshold accounts for the impacts on marine mammal behaviors (feeding, mating and nursing, etc) in the proximity of acoustic activity. These takes or "harassments" are computed using a risk function based on maximum received sound pressure levels (SPL). For a given SPL (above 120 dB re: 1μPa) the risk function is used to estimate the number mammals that will be taken within a given species population [4]. The risk function for odontocetes is plotted in Figure 1A.

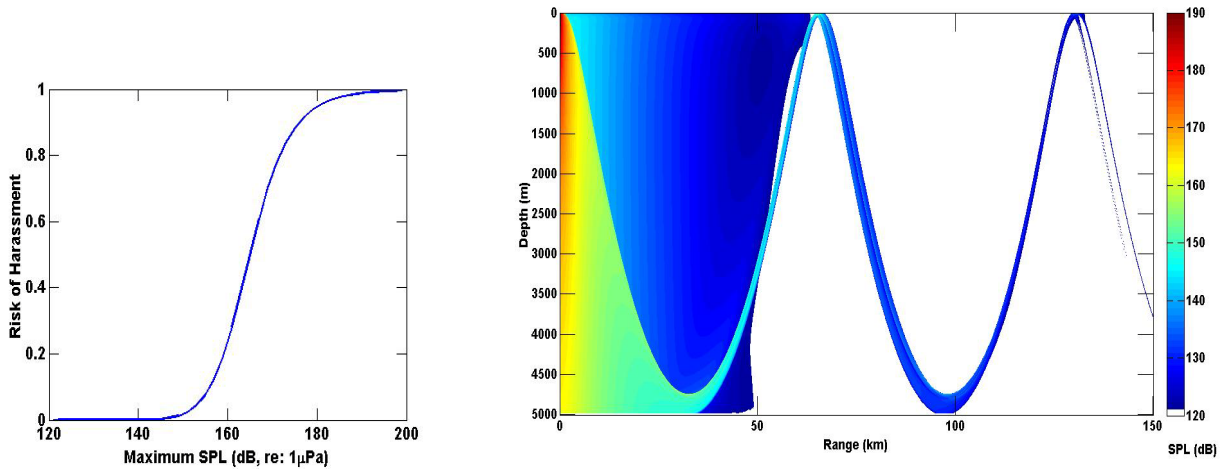

A B

Figure 1. Panel A: The risk function indicates the proportion of a population that is expected to alter its behavior in response to a given maximum SPL. Panel B: Deep ocean SPL values calculated with uniform 5 meter grid spacing. SPL below the basement level of the risk function (120 dB) are not shown. Intensity changes rapidly in some regions near the source and convergence zones, while other relatively large regions have very low intensity levels.

For typical sound sources used in the ocean the SPL may not reach the risk function minimum 120 dB level (representing zero risk) for many kilometers. For this study we consider a typical narrow-band acoustic source at a depth of 10 meters below the ocean surface. The source is omni-directional and emits a single "ping" at a frequency of 3 kHz with intensity of 235 dB relative to 1 micro-Pascal. The water column has a typical deep water sound speed profile ("Munk" profile), extending from the surface to a depth of 5000 meters [5] . To minimize the number of variables we assume the ocean surface is perfectly calm and the bathymetry is flat, so that the entire volume can be represented by a single range-depth transect. The seabed is assumed to be a silty-sand with sound speed of 1550 m/s, density of 1.5 g/cm^3 and attenuation factor of 0.2 dB/wavelength. Figure 1B shows the SPL values calculated using the propagation model Bellhop [2,3] with uniform 5 meter grid spacing. SPL levels below the basement level of the risk function (120 dB) are not shown.

Thus, the combination of the 120 dB low end of the risk function with the source level of many underwater sound sources requires propagation modeling over vast regions of the ocean volume. In addition, we note that the intensity changes rapidly in some regions near the source and convergence zones, while other relatively large regions have very low intensity levels. The AMR method is well-suited to quickly solve such problems which require varying levels of resolution [6]. The AMR technique results in patches of refined grids which are then joined together into larger coarsely sampled grids through interpolation. Therefore, the AMR method allows us to more quickly establish the risk at all points surrounding the sound source. Basing the AMR grid refinement regions on the risk (as opposed to the intensity) allows us to determine the optimal sampling dimensions for the simulation space.

Multiplying the risk by the population distribution provides the number of taken mammals at each point in the simulations space. Evaluation of the total number of takes then provides a metric for comparison of the AMR method with the conventional uniform grid approach. Marine mammals often swim in pods, but for simplicity we will assume them to be distributed uniformly across the ocean's surface with a density of 0.5 mammals/km^2. This density is higher than what is typically observed, but will be used to make the number of takes more meaningful for this simple scenario. Marine mammals may spend a majority of the time near the surface and exhibit a variety of diving behaviors which are unique for each species, but in this example we will assume them to have a uniform distribution in depth down to 2000 meters. Ultimately, this reduced simulation space may be used to run simulations in which movements of simulated animals (animats) can be incorporated for additional accuracy in time-dependent analyses, but these assumptions help generalize and simplify the scenario and more easily compare the two analysis methods.

A closer inspection of the number of takes can also provide a more appropriate boundary for the simulation space. This allows us to determine the maximum extent of the modeled region, with the potential error quantified in terms of marine mammals. We find that the maximum range required for a simulation may be reduced from what would be required by the 120 dB minimum of the risk function.

Finally, we address the issue of sampling in the bearing dimension in environments with rough bathymetry. The conventional approach is to calculate the transmission loss for a fixed number of transects which are spaced uniformly in bearing around the source. The SPL is computed in the range and depth dimensions for each transect and then interpolated for points in-between them. However, without an objective, automated method to distribute the transects around the source there is no way of knowing (1) if islands, sea-mounts or valleys in the bathymetry were ignored because they were contained inside the wedge between the uniformly-spaced transects, or (2) if the number of transects chosen was sufficient to properly sample areas of sloping bathymetry. We are addressing these concerns by first developing an automated procedure to choose transects that intersect these features based on the 2nd derivative of the bathymetry with respect to bearing, and then outlining an algorithm to use the AMR in the bearing dimension.

WORK COMPLETED

Work completed on comparison of current methodologies for preparing impact statements
We completed a series of simulation studies to compare the different animal distribution methods for computing EIS's. The studies held all parameters constant except we changed the calculation of number of harassments depending on whether the static distribution method or animat methods were used. The results were submitted for publication in the Marine Environmental Research Journal.

Work Completed on Adaptive Mesh Refinement of the simulation space
We completed a series of simulation studies to compare the conventional uniform grid method with the AMR method in the range and depth dimensions. The studies held all sound propagation parameters constant and compared the processing time and number of harassments resulting from each gridding method. The number of takes as a function of range was also evaluated. An algorithm to execute the AMR method in the bearing dimension has been outlined, including an automated procedure to ensure that important features in the bathymetry are included in the simulation. Results are shown in the results section. The results were presented at the IEEE Oceans conference, and a paper was published in the conference proceedings. An additional journal publication is in preparation.

RESULTS

Results on Adaptive Mesh Refinement of the simulation space

In this section we evaluate the risk as a function of depth and range using the AMR method and compare the resulting number of takes with the conventional uniform grid approach. A deep ocean and a shallow ocean scenario were each used to compare the two methods. The maximum range required in each scenario is also considered by evaluating the takes as a function of range. Finally, we present a preliminary bathymetry analysis routine to place transects along bearings containing significant bathymetric features, and outline an AMR algorithm to sample the sloping bathymetry between these transects.

Case 1: Deep Ocean

The first case assumes the deep ocean environment described earlier, with convergence zones as shown in figure 1B. The analysis started with grid level 0 using a very coarse spacing of 320 meters (both in range and depth), and then reduced the spacing by ½ for each additional level of the analysis. Figure 2 illustrates the intermediate results in level 4 of the analysis routine. Figure 2A shows the calculated risk for a portion of the level 3 analysis area, from 0 to 4 km in range and 0 to 300 meters in depth with grid spacing of 40 meters. This risk result was then interpolated to a spacing of 20 meters in range and depth to give the risk shown in figure 2B. Next, the SPL was computed at each of these same points and the risk function was used to find the corresponding risk. The level 4 calculated risk is shown in Fig. 2C. Finally, the absolute value of the difference between the level 4 interpolated risk (Fig. 2B) and calculated risk (Fig. 2C) is calculated. Figure 2D shows the grid points where this difference exceeded a risk threshold of 0.1. A new grid is then formed around this subset of points and the process is repeated at level 5 with grid spacing of 10 meters. The process was continued until the grid spacing was reduced to 5 meters, at level 6. The final result is shown in figure 3A, where we note that the risk has diminished nearly to zero for ranges beyond 10 km.

Multiplying the risk in Fig. 3A by the population provides the number of takes at each point. The total number of takes for the entire simulation space was 30.504. The computations were performed on a Dell Optiplex 760 with Intel E8400 3GHz processor with 8 Gb of random access memory, and the total processing time for the AMR analysis was 30.1 seconds. For comparison, Bellhop was also used to calculate the SPL for the entire transect using a spacing of 5 meters, and the risk function was used to calculate the risk at each point. As in the AMR method the risk was multiplied by the population at each point in the grid to get the total number of takes. The uniform grid approach resulted in 30.545 takes after a processing time of 443.8 seconds. The number of takes and processing times for each method are compared in Table 1.

The final risk distribution (Fig. 3A) suggests that calculating the SPL, risk and takes for points that are far from the source may not be an efficient use of computational resources. Figure 3B shows the distribution of takes as a function of range (solid line, left axis). We note that the number of takes near the source is nearly zero and then increases up to a maximum nearly 4km from the source, because the number of takes is the product of the population and risk. Although the SPL near the source is high, the population in the ring area (cylindrical volume) surrounding the source is very small and therefore the number of takes near the source is low. As the range increases the area of each ring surrounding the source also increases and the number of takes goes up. This trend continues until the decreasing SPL overtakes the increase in risk due to larger rings. Eventually, the risk declines to very low levels, causing the number of takes to also decline. Beyond 11 km the number of takes remains very low except near convergence zones (not shown) where it peaks slightly.

The error associated with truncating the range in the simulation is shown as the dashed line (right axis) in figure 3B. Note, that the simulation space could have been reduced from 150 km to 11 km with only a 2 percent error in the final result.

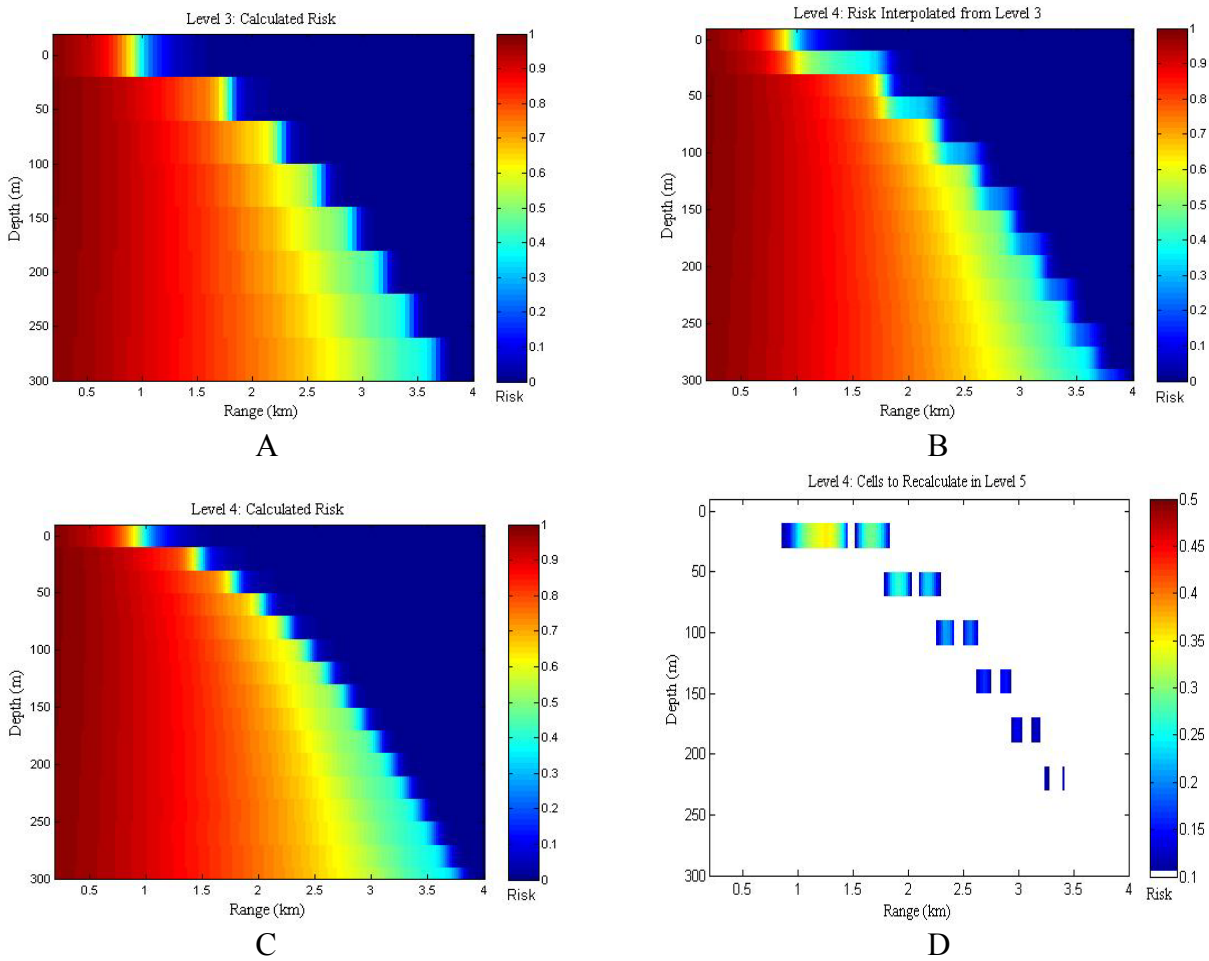

Figure 2. Panel A: The calculated risk for a portion of the level 3 analysis area with grid spacing of 40 meters. Panel B: The risk for a portion of the level 4 analysis area, interpolated from the level 3 analysis area, to a grid spacing of 20 meters. Panel C: The calculated risk for a portion of the level 4 analysis area using a grid spacing of 20 meters. Panel D: The absolute value of the difference between the interpolated risk (Panel B) and the calculated risk (Panel C). Only the grid points where the difference exceeded a risk threshold of 0.1 are shown. These points are then flagged and surrounded by a new smaller analysis area which is evaluated using a finer grid in level 5 of the analysis (not shown).

Table 1. Case 1 (Deep Ocean) comparison of the number of takes and processing times between the AMR method and the conventional uniform grid method. The AMR method arrived at a number of takes that was within 1% of the uniform grid result, 14 times faster than the conventional method.

Case 1 (Deep Ocean)	AMR	Uniform Grid	% Difference
Total Takes	30.504	30.545	0.134 %
Time (sec)	30.1	443.8	93.2 %

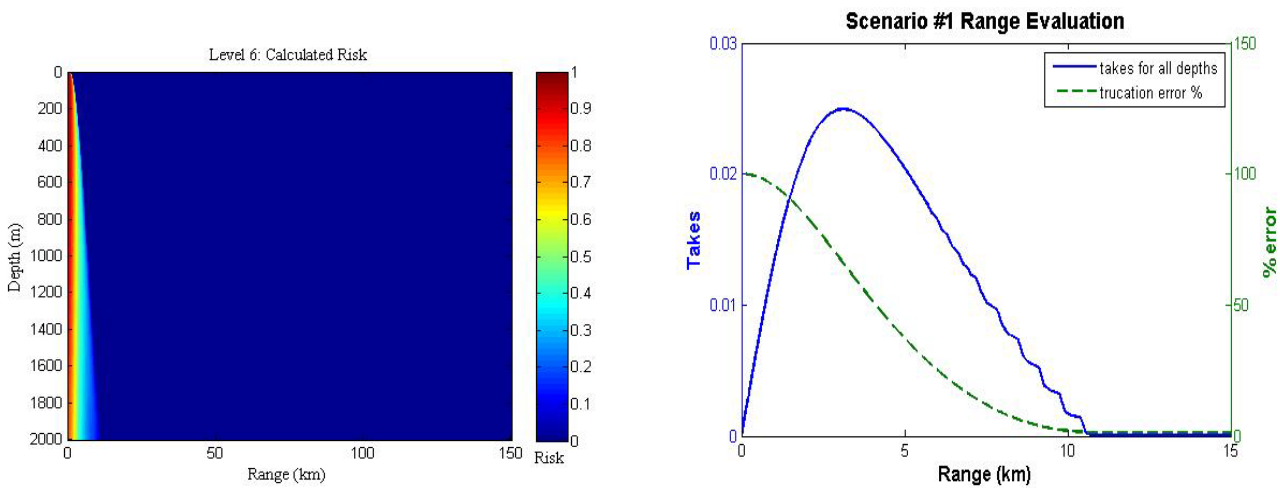

A B

Figure 3. Panel A: The risk values from case 1 (deep ocean) interpolated to a 5 meter grid. Panel B: The distribution of takes as a function of range (solid line, left axis). The risk at each point is multiplied by the population distribution (not shown) to arrive at the number of takes in the simulations space. The error associated with truncating the range in the simulation is also shown (dashed line, right axis). The simulation space could be reduced from 150 km to 11 km with only a 2% error in the final result.

Case 2: Shallow Ocean

The second case assumes the shallow ocean environment extending to a depth of 400 meters using a sound speed profile from AUTEC (Atlantic Undersea Test and Evaluation Center). The resulting surface duct is shown in figure 4A. The AMR method was used to compute the risk using a risk threshold of 1 percent. The risk was then multiplied by the population to provide the number of takes. The total number of takes for the entire simulation space was 99.809, and the total processing time for the AMR analysis was 36.4 seconds. For comparison, Bellhop was again used to calculate the SPL for the entire transect using a spacing of 5 meters, and the risk function was used to calculate the risk at

each point. The uniform grid approach resulted in 102.302 takes after a processing time of 82.3 seconds. The number of takes and processing times for case 2 are compared in Table 2.

Figure 4B shows the distribution of takes as a function of range (solid line, left axis). The error associated with truncating the range in the simulation is shown as the dashed line (right axis) in figure 4B. Note, that the simulation space could have been reduced from 150 km to 50 km with only a 2 percent error in the final result.

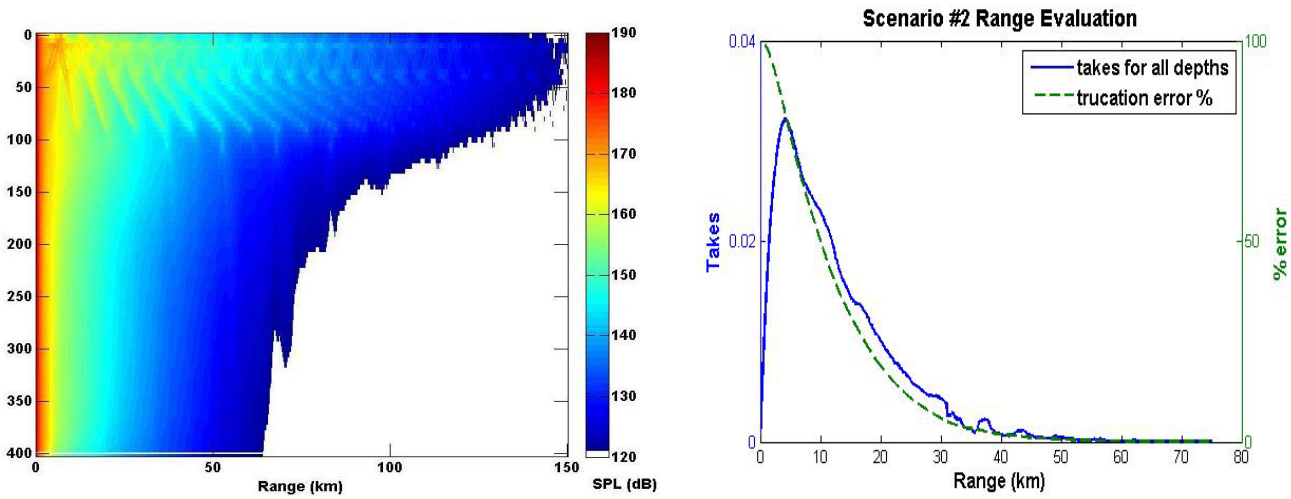

A B

Figure 4. Panel A: Shallow ocean SPL values calculated with uniform 5 meter grid spacing. SPL below the basement level of the risk function (120 dB) are not shown. Panel B: The distribution of takes as a function of range (solid line, left axis). The risk at each point is multiplied by the population distribution (not shown) to arrive at the number of takes in the simulations space. The error associated with truncating the range in the simulation is also shown (dashed line, right axis). The simulation space could be reduced from 150 km to 50 km with only a 2% error in the final result.

Table 2. Case 2 (Shallow Ocean) comparison of the number of takes and processing times between the AMR method and the conventional uniform grid method. The AMR method arrived at a number of takes that was within 2.5% of the uniform grid result, more than 2 times faster than the conventional method.

Case 2 (Shallow Ocean)	AMR	Uniform Grid	% Difference
Total Takes	99.809	102.302	2.44%
Time (sec)	36.356	82.325	55.84%

Optimal Transect placement

The 2nd derivative of the bathymetry with respect to bearing, can be used to identify peaks and valleys in the bathymetry around a source location. As an example we consider a location in the Bahamas with the bathymetry shown in Figure 5A, where land is shown in red and deep ocean valleys are indicated by darker shades of blue. The absolute value of the second derivative of the bathymetry with respect to bearing is shown in figure 5B, where brighter colors represent either peaks or valleys. This provides an objective and automatic method to identify significant bathymetric features at the outset of a simulation. Transects can then be placed along bearing lines that contain such features and after SPL is calculated the risk can be interpolated in regions of sloping bathymetry.

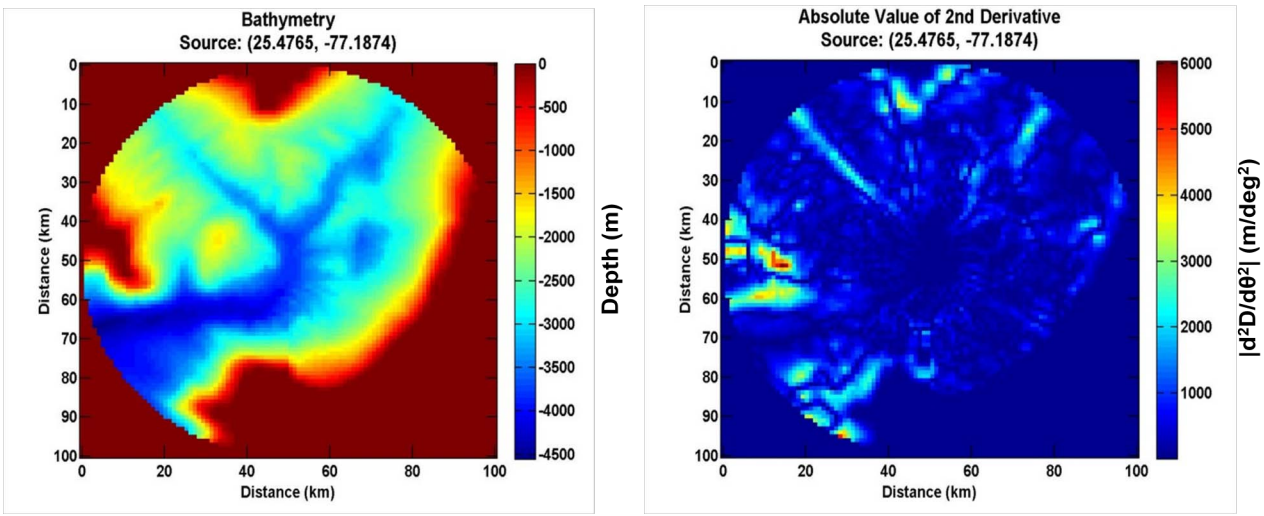

A B

Figure 5. Panel A: The bathymetry for a location near the Bahamas. Panel B: The absolute value of the second derivative of the bathymetry with respect to bearing locates peaks and valleys in the bathymetry.

Adaptive Mesh Refinement algorithm for sampling in the bearing dimension

The results achieved by applying AMR in the range and depth dimensions suggest that AMR may be useful in the bearing dimension as well. An algorithm could be implemented which first calculates the risk for 3 transects – a middle transect and one transect on either side of it. The risk in range and depth could be calculated using the AMR method presented earlier, and forcing the algorithm to stop at a final grid resolution that is the same for all three transects. Next, the two outer transects would be interpolated to form a risk transect at the same bearing as the middle calculated transect. Then comparison of the calculated and interpolated transect would provide an indication of whether additional transects on either side of the middle transect are needed. If the point-by-point differences are large then additional bearings should be evaluated on either side of the center transect. This process would then be repeated until all bearings around the source have been considered and no significant differences remain.

IMPACT/APPLICATIONS

The analysis presented here demonstrate that the AMR method can be used in the range and depth dimensions to quickly and accurately estimate the number of takes in various ocean environments. Evaluation of the resulting number of takes indicates that additional computational time could be saved by limiting the maximum extent of the simulation space. In addition, we address the need for an objective and automated method to distribute transects around the sound source. Finally, we have discussed the need to dynamically place more transects in areas with sloping bathymetry and outlined a method to implement the AMR method in the bearing dimension. These modifications could help speed up calculations in the ESME workbench, making it possible for multiple platforms to be evaluated on a typical personal computer.

TRANSITIONS

None at this time.

RELATED PROJECTS

None at this time.

REFERENCES

[1] D. Houser, "A method for modeling marine mammal movement and behavior for environmental impact assessment," IEEE, J. Ocean. Eng., 31 76-81, 2006.

[2] M. B. Porter, Ocean Acoustics Library, Bellhop, http://oalib.hlsresearch.com/.

[3] M. B. Porter and H. P. Bucker, "Gaussian beam tracing for computing ocean acoustic fields," J. Acoust. Soc. Am. 82(4), 1349–1359 (1987).

[4] U.S. Department of the Navy. "Hawaii Range Complex, Final Environmental Impact Statement/Overseas Environmental Impact Statement" Washington, DC: Department of the Navy, May, 2008.

[5] F.B. Jensen, W.A. Kuperman, M.B. Porter, and H. Schmidt, *Computational Ocean Acoustics*. New York, NY: Springer-Verlag, 2000.

[6] M.J. Berger and P. Colella, "Local Adaptive Mesh Refinement for Shock Hydrodynamics." *Journal of Computational Physics*, vol. 82, pp. 64-84, 1989.

PUBLICATIONS

1. Scott Schecklman, Dorian Houser, Matthew Cross, Dan Hernandez, Martin Siderius, "Comparison of methods used for computing the impact of sound on the marine environment", submitted to *Marine Environmental Research*, (2010).

2. Scott Schecklman, Martin Siderius, and Donald Tornquist, "Computing the effect of sound on the marine environment by the adaptive mesh refinement method", *IEEE Oceans Conference*, Seattle, (2010).

3. David C. Mountain, David Anderson, Andrew Brughera, Matthew Cross, Dorian S. Houser, Nael Musleh, Michael Porter, Martin Siderius, "The ESME Workbench: Simulating the Impact of Anthropogenic Sound on Marine Mammals", The Effects of Noise on Aquatic Life, Second International Conference, Cork Ireland, August (2010).